Chapter 11

# Microwave Absorption by Vortices in Superconductors with a Washboard Pinning Potential

Valerij A. Shklovskij and Oleksandr V. Dobrovolskiy

Additional information is available at the end of the chapter

http://dx.doi.org/10.5772/48358

## 1. Introduction

### 1.1. The essential physical background

It is well-known that a type-II superconductor, while exposed to a magnetic field **B** whose magnitude is between the lower and upper critical field, is penetrated by a flux-line array of Abrikosov vortices, or *fluxons* [1–3]. Each vortex contains one magnetic flux quantum, $\Phi_0 = 2.07 \times 10^{-15}$ Wb, and the repulsive interaction between vortices makes them to arrange in a triangular lattice, with the vortex lattice parameter $a_L \simeq \sqrt{\Phi_0/B}$ where $B = |\mathbf{B}|$. A vortex is often simplified by the hard-core model [4], where the core is a cylinder of normal material with a diameter of the order of the coherence length. In this model, the magnetic field is constant in the core but decays exponentially outside the core over a distance of the order of the effective magnetic penetration depth.

In an ideal material, the vortex array would move with average velocity **v** under the action of the Lorentz force $\mathbf{F}_L$ essentially perpendicular to the transport current. Due to the nonzero viscosity experienced by the vortices when moving through a superconductor, a faster vortex motion corresponds to a larger dissipation. In experiments, inhomogeneities are usually present or can intentionally be introduced in a sample [5] which may give rise to local variations of the superconducting order parameter. This may cause the vortices to be pinned. By this way, the resistive properties of a type-II superconductor are determined by the vortex dynamics, which due to the presence of pinning centers can be described as the motion of vortices in some *pinning potential* (PP) [6]. In particular, randomly arranged and chaotically distributed point-like pinning sites give rise to an ubiquitous, *isotropic* (*i*) pinning contribution, as said of the "background nature". Depending on the relative strength between the Lorentz and pinning forces, the vortex lattice can be either pinned or on move, with a nonlinear transition between these regimes. Thus, the current-voltage characteristics (CVC) of such a sample is strongly nonlinear.

The importance of flux-line pinning in preserving superconductivity in a magnetic field and the reduction of dissipation via control of the vortex motion has been in general recognized since the discovery of type-II superconductivity [1, 2, 7, 8]. Later on, it has been found that the dissipation by vortices can be suppressed to a large degree if the intervortex spacing $a_L$ geometrically matches the period length of the PP [9]. Moreover, artificially created linearly-extended pinning sites are known to be very effective for the reduction of the dissipation by vortices in one [10, 11] or several particular directions. Indeed, if the PP ensued in a superconductor is *anisotropic* (*a*), the direction of vortex motion can be deflected away from the direction of the Lorentz force. In this case, the nonlinear vortex dynamics becomes two-dimensional (2*D*) so that $\mathbf{v} \nparallel \mathbf{F}_L$. The non-collinearity between $\mathbf{v}$ and $\mathbf{F}_L$ is evidently more drastic the weaker the background *i* pinning is [12], which can otherwise mask this effect [13]. The most important manifestation of the pinning anisotropy is known as guided vortex motion, or the *guiding* effect [14], meaning that vortices tend to move along the PP channels rather than to overcome the PP barriers. As a consequence of the guided vortex motion, an *even-in-field* reversal transverse resistivity component appears, unlike the ordinary Hall resistivity which is *odd* regarding the field reversal. A guiding of vortices can be achieved with different sorts of PP landscapes [15, 16] though it is more strongly enhanced and can be more easily treated theoretically when using PPs of the washboard type (WPP).

One more intriguing effect appears when the PP profile is asymmetric. In this case the reflection symmetry of the pinning force is broken and thus, the critical currents measured under current reversal are not equal. As a result, while subjected to an ac current drive of zero mean a net rectified motion of vortices occurs. This is known as a rocking *ratchet* effect and has been widely used for studying the basics of mixed-state physics, e.g., by removing the vortices from conventional superconductors [17], as well as to verify ideas of a number of nanoscale systems, both solid state and biological [18, 19].

## 1.2. Experimental systems with a washboard pinning potential

The first experimental realization of a WPP used a periodic modulation of the thickness of cold-rolled sheets of a Nb-Ta alloy [14]. In this work the influence of isotropic pointlike disorder on the guiding of vortices was discussed for the first time. Later on, lithographic techniques have been routinely employed to create periodic pinning arrays consisting of practically identical nanostructures in the form of, e.g, microholes [20, 21], magnetic dots [22], and stripes [23]. The main idea all these works share is to suppress periodically the superconducting order parameter.

With regard to a theoretical description it has to be stated that a full and exact account of the nonlinear vortex dynamics in superconducting devices proposed in these works [20–23] in a wide range of external parameters is not available due to the complexity of the periodic PP used in these references. Due to this reason it has been proposed by the authors in a number of articles to study a simpler case, such as a WPP periodic in one direction [12, 24–27] or bianisotropic [28]. The main advantage of these approaches implies the possibility to describe the phenomenon of guided vortex motion along the WPP channels, i.e., the directional anisotropy of the vortex velocity, if the transport current is applied under various in-plane angles. For instance, self-organization has been used [10, 29] to provide semi-periodic, linearly extended pinning "sites" by spontaneous facetting of m-plane sapphire substrate surfaces on

which Nb films have been grown. It has been demonstrated that pronounced guiding of vortices occurs. Experimental data [10] were in good agreement with theoretical results [12] that allowed to estimate both, the *i* and *a* PP parameters.

From the viewpoint of theoretical modeling, saw-tooth and harmonic PPs represent the most simple forms of the WPP. On the one hand, these simple forms of the WPP allow one to explicitly calculate the dc magneto-resistivity and the ac impedance tensor as the physical quantities of interest in the problem. On the other hand, these WPP's forms are highly realistic in the sense of appropriate experimental realizations which range from naturally occurring pinning sites in high temperature superconductors (HTSCs) to artificially created linearly-extended pinning sites in high-$T_c$ and conventional superconductors, more often in thin films. Some experimental systems exhibiting a WPP are exemplified in Fig. 1. The experimental geometry of the model discussed below implies the standard four-point bridge of a thin-film superconductor with a WPP placed into a small perpendicular magnetic field with a magnitude $B \ll B_{c2}$ such that our theoretical treatment can be performed in the *single-vortex approximation*.

Summarizing what has been said so far, by tuning the intensity, form, and asymmetry of the WPP in a superconductor, one can manipulate the fluxons via dynamical, directional, and orientational control of their motion. Evidently, a number of more sophisticated phenomena arise due to the variety of the dynamical regimes which the vortex ensemble passes through. In the next sections we will consider a particular problem in the vortex dynamics when the vortices are subjected to superimposed subcritical dc $j_0 < j_c$ and small ac $j_1 \to 0$ current drives at frequencies $\omega$ in the microwave range. What is discussed below can be directly employed to the wide class of thin superconductors with a WPP, including but not limited to those examples shown in Fig. 1. In particular, by looking for the dc magneto-resistivity and the ac impedance responses, we will elucidate: a) how to derive the absorbed power by vortices in such a superconductor as function of all the driving parameters of the problem and b) how to solve the inverse problem, i.e., to reconstruct the coordinate dependence of a PP from the dc current-induced shift in the *depinning* frequency $\omega_p$ [30], deduced from the curves $P(\omega|j_0)$. The importance and further aspects of this issue are detailed next.

### 1.3. Which information can be deduced from microwave measurements?

The measurement of the complex impedance response accompanied by its power absorption $P(\omega)$ in the radiofrequency and microwave range represents a powerful approach to investigate pinning mechanisms and the vortex dynamics in type-II superconductors. The reason for this is that at frequencies $\omega \ll \omega_B$, substantially smaller than those invoking the breakdown of the zero-temperature energy gap ($\omega_B = 2\Delta(0)/\hbar \approx$ 100 GHz for a superconductor with a critical temperature $T_c$ of 10 K), high-frequency and microwave impedance measurements of the mixed state yield information about flux pinning mechanisms, peculiarities in the vortex dynamics, and dissipative processes in a superconductor. It should be stressed that this information can not be extracted from the dc resistivity data obtained in the steady state regime when pinning is strong in the sample. This is due to the fact that in the last case when the critical current density $j_c$ is rather large, the realization of the dissipative mode, in which the flux-flow resistivity $\rho_f$ can be measured, requires $j_0 \gtrsim j_c$. This is commonly accompanied by a non-negligible electron overheating in

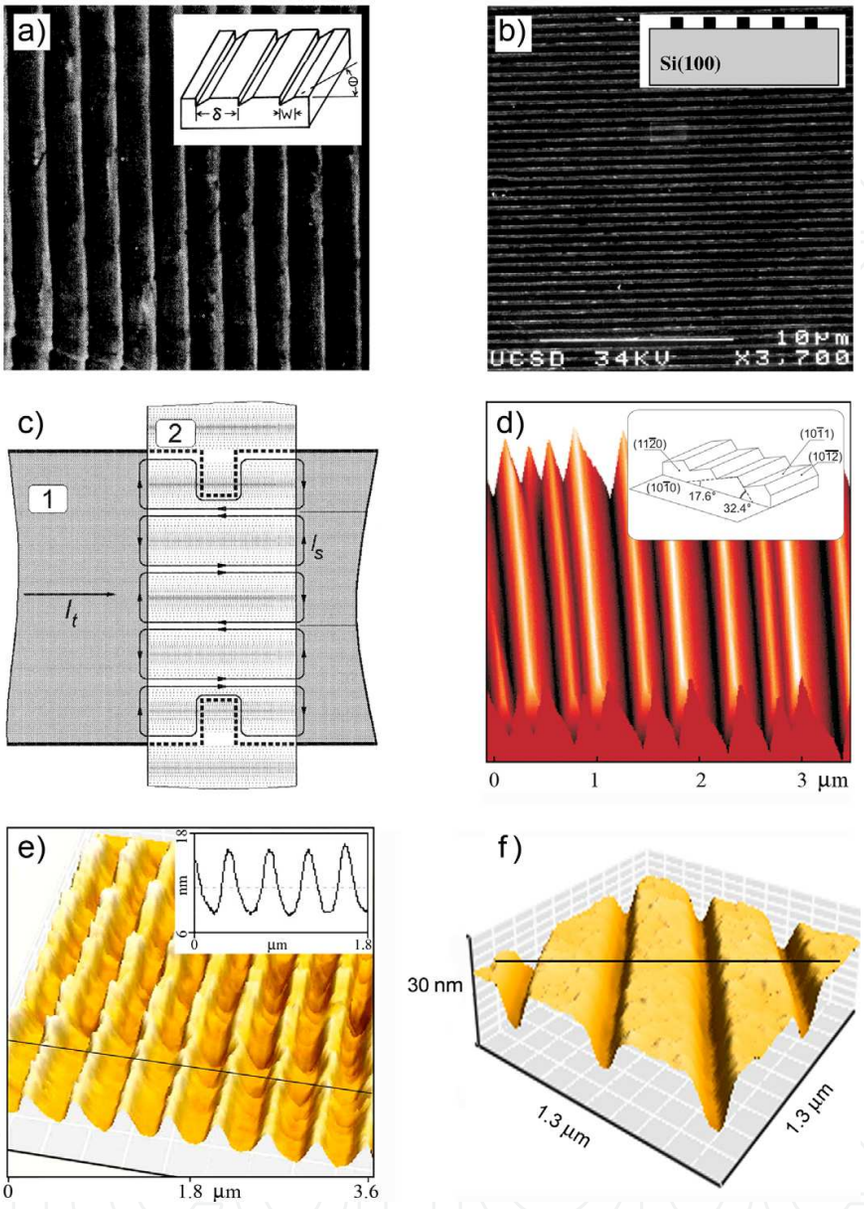


**Figure 1.** Examples of selected experimental systems exhibiting a washboard pinning potential re-printed after original research papers: a) In-2% Bi foil imprinted with diffraction grating [31]. b) Parallel lines of Ni prepared by electron-beam lithography on a Si substrate onto which a Nb film was sputtered [32]. c) Superconducting microbridge (1) with an overlaying magnetic tape (2) containing a pre-recorded magnetization distribution [33]. d) Nb film deposited onto faceted $\alpha - Al_2O_3$ substrate surface [10]. e) Nb film surface with an array of ferromagnetic Co stripes fabricated by focused electron beam-induced deposition [11]. f) Nb film surface with an array of grooves etched by focused electron beam milling [34]. In addition, there is a large number of HTSC-based experimental systems with a WPP, ranging from uniaxially twinned films to the usage of the intrinsic layers within a HTSC [35–39].

the sample [40, 41] which changes the value of the sought $\rho_f$. At the same time, measurements of the absorbed power by vortices from an ac current with amplitude $j_1 \ll j_c$ allow one to determine $\rho_f$ at a dissipative power level of $P_1 \sim \rho_f j_1^2$ which can be many orders of magnitude smaller than $P_0 \sim \rho_f j_0^2$. Consequently, measurements of the complex ac response versus frequency $\omega$ probe the pinning forces virtually in the absence of overheating effects which are otherwise unavoidable at overcritical steady-state dc current densities.

The multitude of experimental works published recently utilizing the usual four-point scheme [42], strip-line coplanar waveguides (CPWs) [43], the Corbino geometry [44, 45], or the cavity method [46] to investigate the microwave vortex response in as-grown thin-film superconductors or in those containing some nano-tailored PP landscape reflects the explosively growing interest in the subject. In connection with this, from the microwave power absorption further insight into the pinning mechanisms can be gained. In particular, artificially fabricated pinning nanostructures provide a PP of unknown shape that requires certain assumptions concerning its coordinate dependence in order to fit the measured data. At the same time, in a real sample a certain amount of disorder is always presented, acting as pinning sites for a vortex as well. By this way, an approach how to reconstruct the form of the PP experimentally realized in a sample is of self-evident importance for both, application-related and fundamental reasons. A scheme how to reconstruct the coordinate dependence of a PP has been recently proposed by the authors [47] and will be elucidated in Sec. 3.3.

### 1.4. Development of the theory in the field

A very early model to describe the absorbed power by vortices refers to the work of Gittleman and Rosenblum (GR) [30]. GR measured the power absorption by vortices in PbIn and NbTa films over a wide range of frequencies $\omega$ and successfully analyzed their data on the basis of a simple model for a $1D$ parabolic PP. In their pioneering work, a small ac excitation of vortices in the absence of a dc current was considered. Later on, GR have supplemented their equation of motion for a vortex with a dc current and have introduced a cosine PP [48]. The GR results have been obtained at $T = 0$ in a linear approximation for the pinning force and will be presented here not only for their historical importance but rather to provide the foundation for the subsequent generalization of the model.

Later on, the theory accounting also for vortex creep at non-zero temperature in a $1D$ cosine PP has been extended by Coffey and Clem (CC) [49]. In the following, the CC theory has been experimentally proved to be very successful [16] to describe the high-frequency electromagnetic properties of superconductors. However, it had been developed for a small microwave current and in the absence of a dc drive.

Recently, the CC results have been substantially generalized by the authors [25, 27] for a $2D$ cosine WPP. The washboard form of the PP allowed for an exact theoretical description of the $2D$ anisotropic nonlinear vortex dynamics for any arbitrary values of the ac and dc current amplitudes, temperature, and the angle between the transport current direction with respect to the guiding direction of the WPP. The influence of the Hall effect and anisotropy of the vortex viscosity on the absorbed power by vortices has also been analyzed [50, 51]. Among other nontrivial results obtained, an enhancement [25] and a sign change [27] in the power absorption for $j_0 \gtrsim j_c$ have been predicted.

Whereas the general *exact* solution of the problem [25, 27] has been obtained for non-zero temperature in terms of a matrix continued fraction [52], here we treat the problem analytically in terms of only elementary functions which allow a more intuitive description of the main effects. Solving the equation of motion for a vortex at $T = 0$, $j_0 < j_c$, and $j_1 \to 0$ in the general case, we also consider some important limiting cases of isotropic vortex viscosity and zero Hall constant provided it substantially helps us to elucidate the physical picture. The theoretical treatment of the problem is provided next.

## 2. General formulation of the problem to be solved

Let the $x$ axis with the unit vector $\mathbf{x}$ (see Fig. 2) be directed perpendicular to the washboard channels, while the $y$ axis with the unit vector $\mathbf{y}$ is along these channels. The equation of motion for a vortex moving with velocity $\mathbf{v}$ in a magnetic field $\mathbf{B} = B\mathbf{n}$, where $B \equiv |\mathbf{B}|$, $\mathbf{n} = n\mathbf{z}$, $\mathbf{z}$ is the unit vector in the $z$ direction,and $n \pm 1$, has the form

$$\hat{\eta}\mathbf{v} + \alpha_H \mathbf{v} \times \mathbf{n} = \mathbf{F} + \mathbf{F}_p, \tag{1}$$

where $\mathbf{F} = (\Phi_0/c)\mathbf{j} \times \mathbf{n}$ is the Lorentz force, $\mathbf{j} = \mathbf{j}_0 + \mathbf{j}_1(t)$, and $\mathbf{j}_1(t) = \mathbf{j}_1 \exp i\omega t$, where $\mathbf{j}_0$ and $\mathbf{j}_1$ are the densities of dc and small ac currents, respectively, and $\omega$ is the ac frequency. $\Phi_0$ is the magnetic flux quantum and $c$ is the speed of light. $\hat{\eta}$ is the vortex viscosity tensor and $\alpha_H$ is the Hall coefficient. In Eq. (1) $\mathbf{F}_p = -\nabla U_p(x)$ is the anisotropic pinning force, where $U_p(x)$ is some periodic pinning potential (PP).

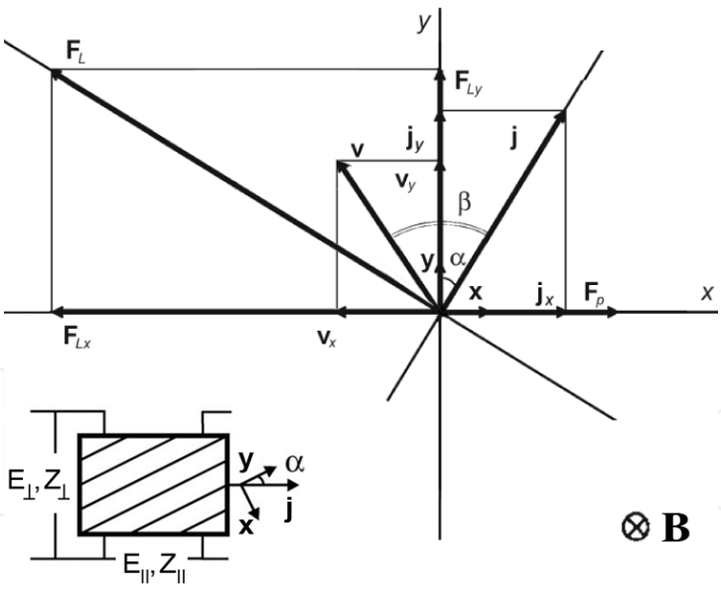


**Figure 2.** The system of coordinates $xy$ with the unit vectors $\mathbf{x}$ and $\mathbf{y}$ is associated with the WPP channels which are parallel to the vector $\mathbf{y}$. The transport current density vector $\mathbf{j} = \mathbf{j}_0 + \mathbf{j}_1 \exp i\omega t$ is directed at an angle $\alpha$ with respect to $\mathbf{y}$. $\beta$ is the angle between the average velocity vector $\mathbf{v}$ and $\mathbf{j}$. $\mathbf{F}_p$ is the average pinning force provided by the WPP and $\mathbf{F}_L$ is the Lorenz force for a vortex. Inset: a schematic sample configuration in the general case. A thin type-II superconductor (foil, thin film, or thin layer of crystal) is placed into a small perpendicular magnetic field $\mathbf{B}$. A WPP is formed in the sample and the direction of the WPP channels is shown by hatching. Experimentally deducible values are the dc voltages $E_\parallel$ and $E_\perp$ as well as the ac impedances $Z_\parallel$ and $Z_\perp$.

If $x$ and $y$ are the coordinates along and across the anisotropy axis, respectively, tensor $\hat{\eta}$ is diagonal in the $xy$ representation, and it is convenient to define $\eta_0$ and $\gamma$ by the formulas

$$\eta_0 = \sqrt{\eta_{xx}\eta_{yy}}, \qquad \gamma = \sqrt{\eta_{xx}/\eta_{yy}}, \qquad \eta_{xx} = \gamma\eta_0, \qquad \eta_{yy} = \eta_0/\gamma, \tag{2}$$

where $\eta_0$ is the averaged viscous friction coefficient, and $\gamma$ is the anisotropy parameter.

Since $U_p(x)$ depends only on the $x$ coordinate and is periodic, i.e., $U_p(x) = U_p(x+a)$, where $a$ is the period of the PP, the pinning force $\mathbf{F}_p$ is directed always along the anisotropy axis $x$ and has no component along the $y$ axis, i.e., $F_{py} = 0$. As usually [25, 27, 48, 49, 53, 54], we use a WPP of the cosine form

$$U_p(x) = (U_p/2)(1 - \cos kx), \tag{3}$$

where $k = 2\pi/a$, $\mathbf{F}_p = -(dU_p/dx)\mathbf{x} = F_{px}\mathbf{x}$, and $F_{px} = -F_c \sin kx$, where $F_c = U_p k/2$ is the maximum value of the pinning force. Because $\mathbf{F} \equiv \mathbf{F}(t) = \mathbf{F}_0 + \mathbf{F}_1(t)$, where $\mathbf{F}_0 = (\Phi_0/c)\mathbf{j}_0 \times \mathbf{n}$ is the Lorentz force invoked by the dc current and $\mathbf{F}_1 = (\Phi_0/c)\mathbf{j}_1(t) \times \mathbf{n}$ is the Lorentz force invoked by the small ac current, we assume that $\mathbf{v}(t) = \mathbf{v}_0 + \mathbf{v}_1(t)$, where $\mathbf{v}_0$ is time-independent, while $\mathbf{v}_1(t) = \mathbf{v}_1 \exp i\omega t$.

Our goal is to determine $\mathbf{v}$ from Eq. (1) and to substitute it then in the expression for the electric field. To accomplish this, Eq. (1) can be rewritten in projections on the coordinate axes

$$\begin{cases} \gamma[v_{0x} + v_{1x}(t)] + \delta[v_{0y} + v_{1y}(t)] = [F_{0x} + F_{1x}(t) + F_{px}]/\eta_0, \\ (1/\gamma)[v_{0y} + v_{1y}(t)] - \delta[v_{0x} + v_{1x}(t)] = [F_{0y} + F_{1y}(t)]/\eta_0, \end{cases} \tag{4}$$

where $\epsilon = \alpha_H/\eta_0$ and $\delta = n\epsilon$.

However, instead of to straightforwardly proceed with the solution of Eqs. (4), we first consider some physically important limiting cases in which Eq. (1) is substantially simplified. Later on, in Sec. 4.3, Eq. (1) will be dealt with in its general form.

## 3. The Gittleman-Rosenblum model

### 3.1. Dynamics of pinned vortices on a small microwave current

Let us consider the case of an isotropic vortex viscosity, i.e., $\gamma = 1$ while $\eta_0 = \eta$ in the absence of Hall effect, i.e., $\epsilon = 0$. We restrict our analysis to the consideration of the vortex motion with velocity $v(t)$ only along the $x$-axis. This case corresponds to $\alpha = 0$ when the vortices move across the PP barriers. Furthermore, we first assume that $j_0 = 0$. Then Eq. (1) can be rewritten in the form originally used [30] for a parabolic pinning potential

$$\eta\dot{x} + k_p x = f_L, \tag{5}$$

where $x$ is the vortex displacement, $\eta$ is the vortex viscosity, $k_p$ is the constant which characterizes the restoring force $f_p$ in the PP well $U_p(x) = (1/2)k_p x^2$ and $f_p = -dU_p/dx = -k_p x$. In Eq. (5) $f_L = (\Phi_0/c)j_1(t)$ is the Lorentz force acting on a vortex, and $j_1(t) = j_1 \exp i\omega t$ is the density of a small microwave current with the amplitude $j_1$. Looking for the solution

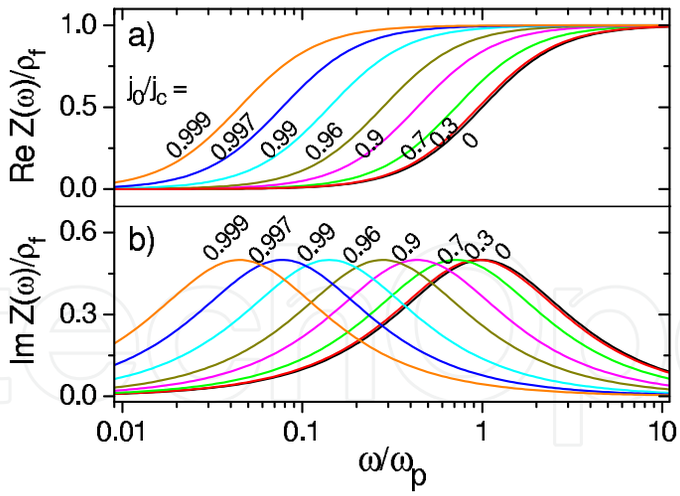


**Figure 3.** The frequency dependences of a) real and b) imaginary parts of the ac impedance calculated for a cosine pinning potential $U_p(x) = (U_p/2)(1 - \cos kx)$ at a series of dc current densities, as indicated. In the absence of a dc current, the GR results are revealed in accordance with Eqs. (9).

of Eq. (5) in the form $x(t) = x \exp i\omega t$, where $x$ is the complex amplitude of the vortex displacement, one immediately gets $\dot{x}(t) = i\omega x(t)$ and

$$x = \frac{(\Phi_0/\eta c) j_1}{i\omega + \omega_p}, \tag{6}$$

where $\omega_p \equiv k_p/\eta$ is the depinning frequency. This frequency $\omega_p$ determines the transition from the non-dissipative to dissipative regimes in the vortex dynamics in response to a small microwave signal, as will be elucidated in the text later. To calculate the magnitude of the complex electric field arising due to the vortex on move, one takes $E = B\dot{x}/c$. Then

$$E(\omega) = \frac{\rho_f j_1}{1 - i\omega_p/\omega} \equiv Z(\omega) j_1. \tag{7}$$

Here $\rho_f = B\Phi_0/\eta c^2$ is the flux-flow resistivity and $Z(\omega) \equiv \rho_f/(1 - i\omega_p/\omega)$ is the microwave impedance of the sample.

In order to calculate the power $P$ absorbed per unit volume and averaged over the period of an ac cycle, the standard relation $P = (1/2)\mathrm{Re}(E \cdot J^*)$ is used, where $E$ and $J$ are the complex amplitudes of the ac electric field and current density, respectively. The asterisk denotes the complex conjugate. Then, from Eq. (7) it follows

$$P(\omega) = (1/2)\mathrm{Re}Z(\omega) j_1^2 = (1/2)\rho_f j_1^2/[1 + (\omega_p/\omega)^2]. \tag{8}$$

For the subsequent analysis, it is convenient to write out real and imaginary parts of the impedance $Z = \mathrm{Re}Z + i\mathrm{Im}Z$, namely

$$\mathrm{Re}Z(\omega) = \rho_f/[1 + (\omega_p/\omega)^2], \qquad \mathrm{Im}Z(\omega) = \rho_f(\omega/\omega_p)/[1 + (\omega/\omega_p)^2]. \tag{9}$$

The frequency dependences (9) are plotted in dimensionless units $Z/\rho_f$ and $\omega/\omega_p$ in Fig. 3 (see the curve for $j_0/j_c = 0$). From Eqs. (5), (6), and (8) it follows that *pinning forces dominate*

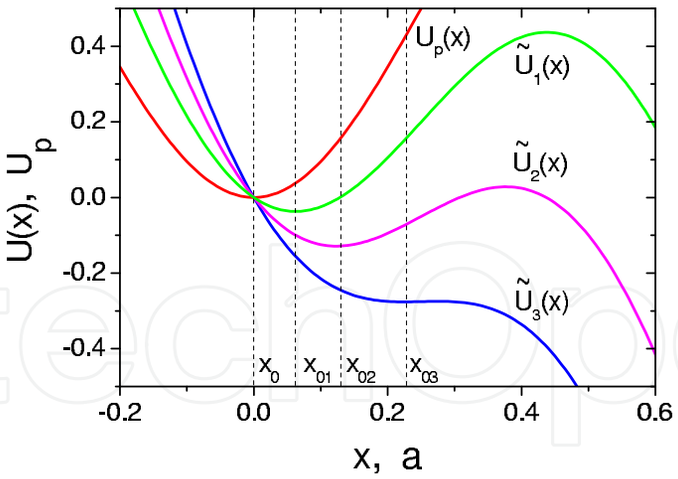


**Figure 4.** Modification of the effective pinning potential $\tilde{U}_i(x) \equiv U_p(x) - f_{0i}x$, where $U_p(x) = (U_p/2)(1 - \cos kx)$ is the WPP, with the gradual increase of $f_0$ such as $0 = f_0 < f_{01} < f_{02} \lesssim f_{03} = f_c$, i.e., a vortex is oscillating in the gradually tilting pinning potential well in the vicinity of the rest coordinate $x_{0i}$.

*at low frequencies*, i.e., when $\omega \ll \omega_p$ and $Z(\omega)$ is mainly nondissipative with $\mathrm{Re}Z(\omega) \approx (\omega/\omega_p)^2 \ll 1$, whereas *frictional forces dominate at higher frequencies*, i.e., when $\omega \gg \omega_p$ and $Z(\omega)$ is dissipative with $\mathrm{Re}Z(\omega) \approx \rho_f[1 - (\omega_p/\omega)^2]$. In other words, due to the reduction of the amplitude of the vortex displacement with the increase of the ac frequency, a vortex is getting not influenced by the pinning force. This can be seen from Eq. (6) where $x \sim 1/\omega$ for $\omega \gg \omega_p$; this is accompanied, however, with the independence of the vortex velocity of $\omega$ in this regime in accordance with Eq. (7).

### 3.2. Influence of a dc current on the depinning frequency

The GR model can be generalized for an arbitrary PP and can also account for an arbitrary dc current superimposed on a small microwave signal. For determinacy, let us consider a subcritical dc current with the density $j_0 < j_c$, where $j_c$ is the critical current density in the absence of a microwave current. Our aim now is to determine to which changes in the effective PP parameters the superimposition of the dc current leads, because $\tilde{U}(x) \equiv U_p(x) - xf_0$ in the presence of $j_0 \neq 0$. Here $U_p(x)$ is the $x$-coordinate dependence of the PP when $j_0 = 0$. The modification of the effective PP with the gradual increase of $f_0$ is illustrated in Fig. 4 for the WPP by Eq. (3). Note also that $f_0 < f_c$, where $f_0$ and $f_c$ are the Lorentz forces which correspond to the current densities $j_0$ and $j_c$, respectively.

In the presence of an arbitrary dc current, the equation of motion for a vortex (5) has the form

$$\eta v(t) = f(t) + f_p, \tag{10}$$

where $f(t) = (\Phi_0/c)j(t)$ is the Lorentz force with $j(t) = j_0 + j_1(t)$, where $j_1(t) = j_1 \exp i\omega t$, and $j_1$ is the amplitude of a small microwave current. Due to the fact that $f(t) = f_0 + f_1(t)$, where $f_0 = (\Phi_0/c)j_0$ and $f_1(t) = (\Phi_0/c)j_1(t)$ are the Lorentz forces for the subcritical dc and microwave currents, respectively, one can naturally assume that $v(t) = v_0 + v_1(t)$, where $v_0$ is time-independent, whereas $v_1(t) = v_1 \exp i\omega t$. In Eq. (10) the pinning force is $f_p =$

$-dU_p(x)/dx$, where $U_p(x)$ is some PP. Our aim is to determine $v(t)$ from Eq. (10) which, taking into account the considerations above, acquires the next form

$$\eta[v_0 + v_1(t)] = f_0 + f_p + f_1(t), \tag{11}$$

Let us consider the case when $j_1 = 0$. If $j_0 < j_c$, i.e., $f_0 < f_c$, where $f_c$ is the maximal value of the pinning force, then $v_0 = 0$, i.e., the vortex is in rest. As it is seen from Fig. 4 the rest coordinate $x_0$ of the vortex in this case depends on $f_0$ and is determined from the condition of equality to zero of the effective pinning force $\tilde{f}(x) = -d\tilde{U}(x)/dx = f_p(x) + f_0$, which reduces to the equation $f_p(x_0) + f_0 = 0$, or

$$f_0 = \frac{dU_p(x)}{dx}|_{x=x_0}, \tag{12}$$

the solution of which is the function $x_0(f_0)$.

Let us now add a small oscillation of the vortex in the vicinity of $x_0$ under the action of the small external alternating force $f_1(t)$ with the frequency $\omega$. For this we expand the effective pinning force $\tilde{f}(x)$ in the vicinity of $x = x_0$ into a series in terms of small displacements $u \equiv x - x_0$ which gives

$$\tilde{f}(x - x_0) \simeq \tilde{f}(x_0) + \tilde{f}'(x_0)u + \dots \tag{13}$$

Then, taking into account that $\tilde{f}(x_0) = 0$ and $\tilde{f}'(x_0) = U_p''(x_0)$, Eq. (11) acquires the form

$$\eta\dot{u}_1 + \tilde{k}_p u = f_1, \tag{14}$$

where $\tilde{k}_p(x_0) = U_p''(x_0)$ is the effective constant characterizing the restoring force $\tilde{f}(u)$ at small oscillations of a vortex in the effective PP $\tilde{U}(x)$ close by $x_0(f_0)$, and $v_1 = \dot{u} = i\omega u$. Equation (14) for the determination of $v_1$ is physically equivalent to GR Eq. (5) with the only distinction that the vortex depinning frequency $\tilde{\omega}_p \equiv \tilde{k}_p/\eta$ now depends on $f_0$ through Eq. (12), i.e., on the dc transport current density $j_0$. Thereby, all the results of Sec. 3.1 [see Eqs. (6)-(9)] can be repeated here with the changes $x \to u$ and $\omega_p \to \tilde{\omega}_p$. It should be noted, that all the described till now did not require one to know the actual form of the PP. In order to discuss the changes in the dependences $\mathrm{Re}Z(\omega)$ and $\mathrm{Im}Z(\omega)$ caused by the dc current, the PP must be specified. We take the cosine WPP determined by Eq. (3); though any other non-periodic PP can also be used. For the curves $\mathrm{Re}Z(\omega|j_0)$ and $\mathrm{Im}Z(\omega|j_0)$ plotted in Fig. 3, the dependence $\tilde{\omega}_p(j_0/j_c) = \omega_p\sqrt{1-(j_0/j_c)^2}$ for the cosine WPP is used [50]. Its derivation will also be outlined in Sec. 3.3.

Now we turn to the discussion of the figure data from which it is evident that with increase of $j_0$ the curves $\mathrm{Re}Z(\omega|j_0)$ and $\mathrm{Im}Z(\omega|j_0)$ shift to the left. The reason for this is that with increase of $j_0$ the PP well while tilted is broadening, as illustrated in Fig. 3. Thus, during the times shorter than $\tau_p = 1/\omega_p$, i.e., for $\omega > \omega_p$, a vortex can no longer non-dissipatively oscillate in the PP's well. As a consequence, the enhancement of $\mathrm{Re}Z(\omega)$ occurs at lower frequencies. At the same time, the curves in Fig. 3 maintain their original shape. Thus, *the only universal parameter to be found experimentally is the depinning frequency* $\omega_p$. For a fixed frequency and different $j_0$, real part of $Z(\omega)$ always acquires larger values for larger $j_0$, whereas the maximum in imaginary part of $Z(\omega)$ precisely corresponds to the middle point

of the nonlinear transition in $\mathrm{Re}Z(\omega)$. It should be noted that in the presence of $j_0 \neq 0$ *the dissipation remains non-zero* even at $T = 0$, though it is very small at very low frequencies.

### 3.3. Reconstruction of a pinning potential from the microwave absorption data

*3.3.1. General scheme of the pinning potential reconstruction*

We now turn to the detailed analytical description how to reconstruct the coordinate dependence of a PP experimentally ensued in the sample, on the basis of microwave power absorption data in the presence of a subcritical dc transport current. It will be shown that from the dependence of the depinning frequency $\tilde{\omega}_p(j_0)$ as a function of the dc transport current $j_0$ one can determine the coordinate dependence of the PP $U_p(x)$. The physical background for the possibility to solve such a problem is Eq. (12) which gives the correlation of the vortex rest coordinate $x_0$ with the value of the static force $f_0$ acting on the vortex and arising due to the dc current $j_0$.

From Eq. (12) it follows that while increasing $f_0$ from zero up to its critical value $f_c$ one in fact "probes" all the points in the dependence $U_p(x)$. Taking the $x_0$-coordinate derivative in Eq. (12), one obtains

$$dx_0/df_0 = 1/U_p''(x_0) = 1/\tilde{k}_p(x_0), \tag{15}$$

where the relation $U''(x_0) = \tilde{k}_p(x_0)$ has been used [see Eq. (14) and the text below]. By substituting $x_0 = x_0(f_0)$, Eq. (15) can be rewritten as $dx_0/df_0 = 1/\tilde{k}_p[x_0(f_0)]$, and thus,

$$\frac{dx_0}{df_0} = \frac{1}{\eta\tilde{\omega}_p(f_0)}. \tag{16}$$

If the dependence $\tilde{\omega}(f_0)$ has been deduced from the experimental data, i.e., fitted by a known function, then Eq. (16) allows one to derive $x_0(f)$ by integrating

$$x_0(f_0) = \frac{1}{\eta}\int_0^{f_0} \frac{df}{\tilde{\omega}_p(f)}. \tag{17}$$

Then, having calculated the inverse function $f_0(x_0)$ to $x_0(f_0)$ and using the relation $f_0(x_0) = U_p'(x_0)$, i.e., Eq. (12), one finally obtains

$$U_p(x) = \int_0^x dx_0 f_0(x_0). \tag{18}$$

*3.3.2. Example procedure to reconstruct a pinning potential*

Here we would like to support the above-mentioned considerations by giving an example of the reconstruction procedure for a WPP. Let us suppose that a series of power absorption curves $P(\omega)$ has been measured for a set of subcritical dc currents $j_0$. Then for determinacy, let us imagine that each $i-$curve of $P(\omega|j_0)$ like those shown in Fig. 3 has been fitted with its fitting parameter $\tilde{\omega}_p$ so that one could map the points $[(\tilde{\omega}_p/\omega_p)_i, (j_0/j_c)_i]$, as shown by triangles in Fig. 5.

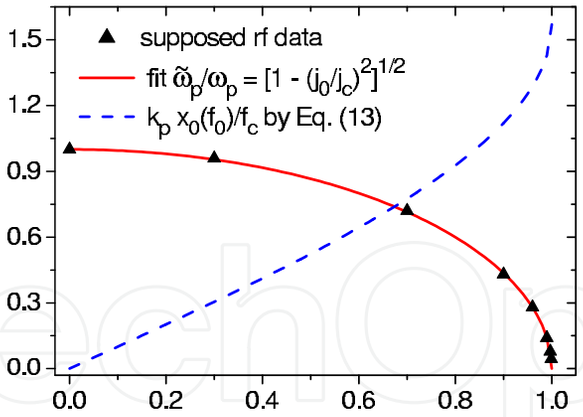


**Figure 5.** The pinning potential reconstruction procedure: step 1. A set of $[(\tilde{\omega}_p/\omega_p)_i, (j_0/j_c)_i]$ points (▲) has been deduced from the supposed measured data and fitted as $\tilde{\omega}_p/\omega_p = \sqrt{1-(j_0/j_c)^2}$ (solid line). Then by Eq. (17) $x_0(f_0) = (f_c/k_p)\arcsin(f_0/f_c)$ (dashed line).

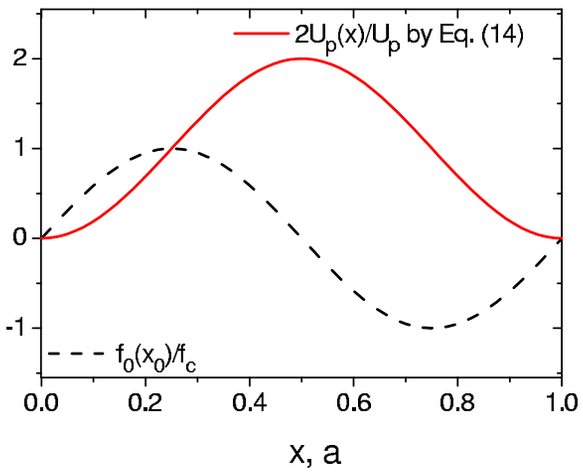


**Figure 6.** The pinning potential reconstruction procedure: step 2. The inverse function to $x_0(f_0)$ is $f_0(x_0) = f_c \sin(x_0 k_p/f_c)$ (dashed line). Then by Eq. (18) $U_p(x) = (U_p/2)(1-\cos kx)$ is the PP sought (solid line).

We fit the figure data in Fig. 5 by the function $\tilde{\omega}_p/\omega_p = \sqrt{1-(j_0/j_c)^2}$ and then substitute it into Eq. (17) from which one calculates $x_0(f_0)$. In the case, the function has a simple analytical form, namely $x_0(f_0) = (f_c/k_p)\arcsin(f_0/f_c)$. Evidently, the inverse to it function is $f_0(x_0) = f_c \sin(x_0 k_p/f_c)$ with the period $a = 2\pi f_c/k_p$ (see also Fig. 6). By taking the integral (18) one finally gets $U_p(x) = (U_p/2)(1-\cos kx)$, where $k = 2\pi/a$ and $U_p = 2f_c^2/k_p$.

### 3.4. Concluding remarks on the reconstruction scheme of a pinning potential

The problem to reconstruct the actual form of a potential subjected to superimposed constant and small alternation perturbations arises not only in the vortex physics but also in related fields such as charge-density-wave pinning [55] and Josephson junctions [56]. In the vortex physics, an early scheme how to reconstruct the coordinate dependence of the pinning force from measurements implying a small ripple magnetic field superposed on a larger dc magnetic field had been previously reported [57]. Also, due to the closest mathematical analogy should be also mentioned the Josephson junction problem wherein a plenty of

non-sine current-phase relations is known to occur [56] and which could in turn benefit from the results reported here.

A respective experiment can be carried out at $T \ll T_c$ and implies a small microwave current density $j_1 \ll j_c$. Though the potential reconstruction scheme has been exemplified for a cosine WPP, i.e., for a periodic and symmetric PP, single PP wells [43] can also be proven in accordance with the provided approach. In the general case, *the elucidated here procedure does not require periodicity of the potential and can account also for asymmetric ones*. If this is the case, one has to perform the reconstruction procedure under the dc current reversal, i.e., two times: for $+j_0$ and $-j_0$.

Here, our consideration was limited to $T = 0$, $j_0 < j_c$, and $j_1 \to 0$ because this has allowed us to provide a clear reconstruction procedure in terms of elementary functions accompanying with a simple physical interpretation. Experimentally, adequate measurements can be performed, i.e., on conventional thin-film superconductors (e.g., Nb, NbN) at $T \ll T_c$. These are suitable due to substantially low temperatures of the superconducting state and that relatively strong pinning in these materials allows one to neglect thermal fluctuations of a vortex with regard to the PP's depth $U_p \simeq 1000 \div 5000$ K [10]. It should be stressed that due to the universal form of the dependences $P(\omega|j_0)$, the depinning frequency $\omega_p$ plays a role of the only fitting parameter for each of the curves $P(\omega|j_0)$, thus fitting of the measured data seems to be uncomplicated. However, one of most crucial issues for the experiment is to adequately superimpose the applied currents and then, to uncouple the picked-up dc and microwave signals maintaining the matching of the impedances of the line and the sample. Quantitatively, experimentally estimated values of the depinning frequency in the absence of a dc current at a temperature of about $0.6T_c$ are $\omega_p \approx 7$ GHz for a 20 nm-thick [45] and a 40 nm-thick [46] Nb films. This value is strongly suppressed with increase of both, the field magnitude and the film's thickness.

Concerning the general validity of the results obtained, one circumstance should be recalled. The theoretical consideration here has been performed in the single-vortex approximation, i.e., is valid only at small magnetic fields $B \ll B_{c2}$, when the distance between two neighboring vortices, i.e., the period of a PP is larger as compared with the effective magnetic field penetration depth, $a \gtrsim \lambda$.

## 4. Solution of the problem in the general case

### 4.1. General remarks on the Hall parameter and anisotropy of the vortex viscosity

Now, the extent to which the Hall term in the equation of motion of the vortex and a possible anisotropy of the viscous term affect the $2D$ dynamics and the resistive properties of the vortex ensemble both, at a direct (subcritical) current and at a small microwave ac current, will be investigated. It should be pointed out that, even though the Hall angle $\theta_H$ and, consequently, the dimensionless Hall coefficient $\epsilon$ is small for most superconductors, i.e., $\epsilon \ll 1$, anomalously large values of $\epsilon$ are observed in YBCO, $NbSe_2$, and Nb films in a number of cases at sufficiently low temperatures [58]; i.e., $\tan\theta_H \geq 1$. In the absence of pinning (Sec. 4.2), this means that the vortex velocity $\mathbf{v}$ in this case is directed predominantly along the direction of $\mathbf{j}_1(t)$, whereas, with a small Hall angle ($\tan\theta_H$), the directions of $\mathbf{v}$ and $\mathbf{j}_1(t)$ are virtually orthogonal. The influence of the Hall term on the vortex dynamics is

taken into consideration because, as will be shown below, the absorption by vortices at an ac current substantially depends on both the magnitude of $\epsilon$ and the frequency $\omega$, and angle $\alpha$. Moreover, the analysis shows that the resistive characteristics of a sample at a subcritical dc is independent of the value of the Hall constant. In other words, it is impossible to extract the value of $\epsilon$ from experimental data at a dc, while $\epsilon$ *can be determined from an analysis of the power absorption at an ac* (Sec. 4.3). The physical cause of such a behavior of the transverse resistive response at a subcritical dc current is associated with the suppression of the Hall response as a consequence of vortex pinning in the transverse with respect to the WPP channels direction of their possible motion.

The viscosity anisotropy is taken into consideration because the anisotropy in the *ab* plane is fairly large in most HTSC crystals: for example, for YBCO crystals, the magneto-resistivity as the vortices move along the *a* or *b* axis can differ by more than a factor of 2 [35].

## 4.2. The case of zero pinning strength and arbitrary currents

*4.2.1. Computing the dc resistivities*

Let the Hall constant now be arbitrary ($\epsilon \neq 0$), while the vortex viscosity is arbitrary and anisotropic ($\gamma \neq 1$). We first consider the $2D$ vortex motion in the absence of pinning, i.e., when $\mathbf{F}_p = 0$. Note, that both the dc and the microwave ac currents are of arbitrary densities. The equation of motion for a vortex has the form

$$\hat{\eta}\mathbf{v} + \alpha_H \mathbf{v} \times \mathbf{n} = \mathbf{F}. \tag{19}$$

In this case, projections of the vortex velocity on the $xy$ axes at constant current are $v_{0x} = \tilde{F}_{0x}/\tilde{\eta}_0$ and $v_{0y} = \tilde{F}_{0y}/\tilde{\eta}_0$, where $\tilde{\eta}_0 = \eta_0\gamma(1+\delta^2)$, $\tilde{F}_{0x} = F_{0x} - \gamma\delta F_{0y}$, and $\tilde{F}_{0y} = \gamma^2 F_{0y} + \gamma\delta F_{0x}$. The main physical quantity that makes is possible to determine the resistive characteristics of the sample, i.e., its dc resistivity tensor $\hat{\rho}_0$ and the ac impedance tensor $\hat{Z}_1$ at frequency $\omega$, is the electric field $\mathbf{E}(t)$ induced by the moving vortex system

$$\mathbf{E}(t) = [\mathbf{B} \times \mathbf{v}(t)]/c = (nB/c)[-v_y(t)\mathbf{x} + v_x(t)\mathbf{y}]. \tag{20}$$

We note that $\mathbf{E}(t) = \mathbf{E}_0 + \mathbf{E}_1(t)$, where $\mathbf{E}_0$ is the dc electric field, while $\mathbf{E}_1(t) = \mathbf{E}_1 \exp i\omega t$, where $\mathbf{E}_1$ is the complex amplitude of the ac electric field $\mathbf{E}_1(t)$. We next recall that the experimentally measurable resistive responses (longitudinal $E_\parallel$ and transverse $E_\perp$ with respect to the current direction) are associated with the responses $E_x$ and $E_y$ in the $xy$ coordinate system by the relations $E_\parallel = E_x \sin\alpha + E_y \cos\alpha$ and $E_\perp = -E_x \cos\alpha + E_y \sin\alpha$, where $E_x = -n(B/c)v_y$ and $E_y = n(B/c)v_x$. At dc current, $E_{0\parallel}$ and $E_{0\perp}$ are respectively determined by

$$\begin{cases} E_{0\parallel} = [\rho_f j_0/\gamma\Delta](\gamma^2 \sin^2\alpha + \cos^2\alpha) \equiv j_0\rho_{0\parallel}, \\ E_{0\perp} = [\rho_f j_0/\gamma\Delta](\gamma\delta + (1-\gamma^2)\sin\alpha\cos\alpha) \equiv j_0\rho_{0\perp}, \end{cases} \tag{21}$$

where $\rho_f \equiv B\Phi_0/\eta_0 c^2$ is the flux-flow resistivity and $\Delta = 1 + \delta^2$. Separating the even and odd in $n$ components in Eqs. (21) one finally obtains

$$\begin{array}{ll} \rho^+_{0\parallel} = (\rho_f/\gamma\Delta)(\gamma^2\sin^2\alpha + \cos^2\alpha), & \rho^-_{0,\parallel} = 0, \\ \rho^+_{0\perp} = (\rho_f/\gamma\Delta)(1-\gamma^2)\sin\alpha\cos\alpha, & \rho^-_{0\perp} = \rho_f\delta/\Delta. \end{array} \tag{22}$$

It should be pointed out that Eqs. (22) are independent of $j_0$, i.e., the corresponding dc CVCs are *linear*. In other words, all three nonzero resistive responses correspond to the *flux-flow* regime of the vortex dynamics. The difference between them consists only in different dependences of the magnetoresistivities $\rho_{0\parallel}^{+}$, $\rho_{0\perp}^{+}$, and $\rho_{0\perp}^{-}$ on parameters $\alpha$, $\gamma$, and $\epsilon$. The presence of pinning (see Sec. 4.3.1) substantially changes these final conclusions.

*4.2.2. Limiting cases of isotropic viscosity and/or zero Hall constant*

Let us now consider several simple, physically different limiting cases which follow from Eq. (22). If there is no viscosity anisotropy ($\gamma = 1$) and no Hall effect ($\epsilon = 0$), the vortex dynamics is isotropic, i.e., is independent of the angle $\alpha$. In this case, the vortex dynamics corresponds to the flux-flow mode which is *independent of the field reversal*. As expected, the only nonzero component is $\rho_{0\parallel}^{+} = \rho_f$ which is even with respect to the change $\mathbf{B} \to -\mathbf{B}$.

However, if $\gamma = 1$ and only the Hall effect $\epsilon \neq 0$ is to be considered, the vortex dynamics becomes anisotropic in the sense that the directions of $\mathbf{F}_0$ and $\mathbf{v}_0$ no longer coincide. This *odd-in-field* anisotropy is of a Hall origin and can be quantitatively characterized by the Hall angle, $\theta_H$, determined as

$$\tan\theta_H = \rho_{0\perp}^{-}/\rho_{0\parallel}^{+} = \delta, \tag{23}$$

where $\rho_{0\perp}^{-}$ is the new transverse odd (Hall) component of the magneto-resistivity. If $|\delta| \ll 1$, the Hall anisotropy is weak, and the vortex velocity $\mathbf{v}_0$ is virtually perpendicular to the dc density $\mathbf{j}_0$, whereas, if $|\delta| \gg 1$, the directions of $\mathbf{v}_0$ and $\mathbf{j}_0$ virtually coincide.

The presence of a viscosity anisotropy $\gamma \neq 1$ even in the absence of the Hall effect ($\epsilon = 0$) results in the appearance of one more new magneto-resistivity $\rho_{0\perp}^{+}$. This component is even with respect to the inversion $\mathbf{B} \to -\mathbf{B}$ and, like the Hall effect, causes the vortex motion to be anisotropic, i.e., it causes the directions of $\mathbf{F}_0$ and $\mathbf{v}_0$ not to coincide. It is convenient to characterize the corresponding *even-in-field* anisotropy by the angle $\beta$ defined as

$$\cot\beta = -\rho_{0\perp}^{+}/\rho_{\parallel}^{+} = (\gamma^2 - 1)/(\gamma^2\tan\alpha + \cot\alpha). \tag{24}$$

By analogy with the appearance of directed motion of the vortices in the presence of a WPP, when there is no Hall effect and no viscosity anisotropy, the angle $\beta$ defined by Eq. (24) can be treated similarly to that for the guiding effect in the problem with pinning.

*4.2.3. Computing the ac impedance*

Carrying out an analysis for ac current in the same way like for dc current, one has $v_{1x}(t) = \tilde{F}_{1x}(t)/\tilde{\eta}_0$ and $v_{1y}(t) = \tilde{F}_{1y}(t)/\tilde{\eta}_0$, where $\tilde{F}_{1x}(t) = F_{1x} - \gamma\delta F_{1y}$, and $\tilde{F}_{1y}(t) = \gamma^2 F_{1y} + \gamma\delta F_{1x}$. Then

$$\begin{cases} E_{1\parallel} = [\rho_f j_1(t)/\gamma\Delta](\gamma^2\sin^2\alpha + \cos^2\alpha) \equiv j_1(t)Z_{\parallel}, \\ \\ E_{1\perp} = [\rho_f j_1(t)/\gamma\Delta](\gamma\delta + (1-\gamma^2)\sin\alpha\cos\alpha) \equiv j_1(t)Z_{\perp}. \end{cases} \tag{25}$$

Longitudinal ($\parallel$) and transverse ($\perp$) components are determined here with respect to the direction of $\mathbf{j}_1$. Separating the even and odd with respect to $n$ components in Eqs. (25), one

finally gets

$$Z_{\parallel}^{+} = (\rho_f/\gamma\Delta)(\gamma^2 + \sin^2\alpha + \cos^2\alpha), \qquad Z_{\parallel}^{-} = 0,$$
$$Z_{\perp} = (\rho_f/\gamma\Delta)(1-\gamma^2)\sin\alpha\cos\alpha, \qquad Z_{\perp}^{-} = \rho_f\delta/\Delta. \tag{26}$$

It should be pointed out that, as it can be seen from Eqs. (26) and (22), the relationships for the transverse and longitudinal resistive responses at dc current formally coincide with those for the corresponding impedances in the absence of pinning, i.e., the impedance components are *real*. However, it should be recalled that $\rho_{\parallel,\perp} = \mathrm{Re}[Z_{\parallel,\perp}\exp i\omega t]$.

*4.2.4. Microwave absorption by vortices in the absence of pinning*

To compute the absorbed power $P$ in the ac response per unit volume and averaged over the period of an ac cycle, we use the standard expression $P = (1/2)\mathrm{Re}(\mathbf{E}_1 \cdot \mathbf{j}_1^*)$, where $\mathbf{E}_1$ and $\mathbf{j}_1$ are the complex amplitudes of the ac electric field and the current density, respectively. Then, using Eqs. (25), it can be shown that

$$P = (j_1^2/2)\bar{\rho} \equiv (j_1^2/2)\mathrm{Re}Z_{\parallel} = P_0(\gamma^2\sin^2\alpha + \cos^2\alpha)/\gamma\Delta, \tag{27}$$

where $P_0 = \rho_f(j_1^2/2)$. When $\gamma = 1$, the absorbed power becomes isotropic and depends only on the dimensionless Hall constant $\epsilon$, i.e., $P = P_0/\Delta$ with $P$ decreasing as $\epsilon$ increases. This is physically associated with the already established fact that, as $\epsilon$ increases, the direction of vector $\mathbf{v}_1$ approaches closer and closer to the direction of vector $\mathbf{j}_1$, so that the corresponding component of the longitudinal ac electric field $E_{1\parallel}$ decreases in amplitude as $\theta_H$ increases, while the absorbed power falls off. According to the physical picture and as it follows from Eq. (27), the power absorption is maximal and equals $P_0$ when $\gamma = 1$ and $\epsilon = 0$.

However, if $\gamma \neq 1$ and $\epsilon \neq 0$, one has $P = P(\alpha, \gamma, \epsilon)$, i.e., the absorbed power is anisotropic. Figure 7 shows the dependence of $P/P_0$ as a function of the anisotropy parameter $\gamma$ at the Hall parameter $\delta = 0.1$ for various values of the angle $\alpha$. It follows from Eq. (27) that the influence of parameter $\epsilon$ on $P(\alpha, \gamma, \epsilon)$ for any $\alpha$ and $\gamma$ reduces to a reduction of the absorption with increasing $\epsilon$, as well as the fact that the absorption anisotropy when $\gamma \neq 1$ is determined by the value of the nonlinear with respect to $\alpha$ and $\gamma$ combination $\gamma\sin^2\alpha + (1/\gamma)\cos^2\alpha$. The latter implies that the term $(1/\gamma)\cos^2\alpha$ increases as $\alpha \to 0$ and $\gamma \to 0$, and that the term $\gamma\sin^2\alpha$ increases as $\alpha \to \pi/2$ and $\gamma \gg 1$. All these features are easy to see in Fig. (7).

## 4.3. The case of arbitrary pinning strength and subcritical currents

*4.3.1. Computing the dc resistivities*

Let us first consider the case in which there is no ac current, i.e., $j_1 = 0$. It then follows from Eq. (4) that

$$\begin{cases} \gamma v_{0x} + \delta v_{0y} = (F_{0x} + F_{px})/\eta_0, \\ (1/\gamma)v_{0y} - \delta v_{0x} = F_{0y}/\eta_0. \end{cases} \tag{28}$$

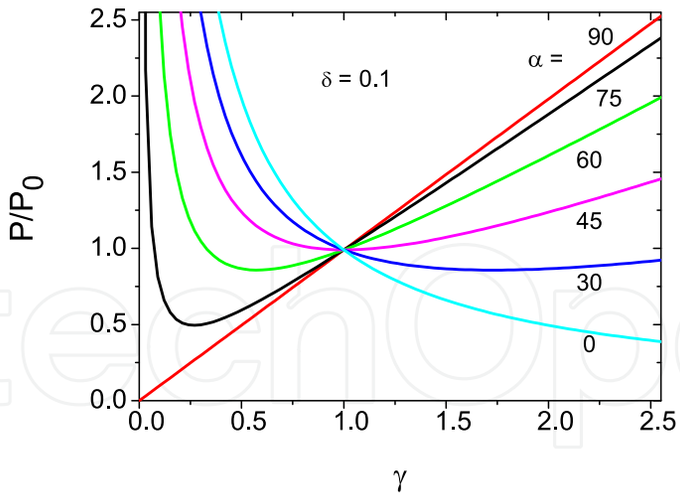


**Figure 7.** Dependence of the absorbed power $P/P_0$ on the anisotropy parameter $\gamma$ at the Hall parameter $\delta = 0.1$ for a series of values of the angle $\alpha$, as indicated.

The solution of this system of equation is

$$v_{0x} = (\tilde{F}_{0x} + F_{px})/\tilde{\eta}_0, \qquad v_{0y} = \gamma F_{0y}/\tilde{\eta}_0 + \gamma\delta(\tilde{F}_{0x} + F_{px})/\tilde{\eta}_0. \tag{29}$$

The motion of a vortex along the $x$ axis will differ, depending on the values of the anisotropy parameter $\gamma$, the Hall coefficient $\epsilon$, and the force $\tilde{F}_{0x}$. If $\tilde{F}_{0x} < F_c$, the vortex comes to rest in this direction, i.e., $V_{0x} = 0$. As follows from Fig. 4, the vortex's rest coordinate $x_0$ in this case depends on the value of $\tilde{F}_{0x}$. It then follows from Eq. (29) that, to determine the dependence $x_0(\tilde{F}_{0x})$, it is necessary to solve the equation $\tilde{F}_{0x} + F_{px} = 0$. For the WPP given by Eq. (3), the solution is

$$x_0 = (1/k)\arcsin(\tilde{F}_{0x}/F_c), \tag{30}$$

where $\tilde{F}_{0x}/F_c = \tilde{j}_{0y}/j_c$, $\tilde{j}_{0y} = n(j_{0y} + \gamma\delta j_{0x})$, and $j_c$ is the critical current when $\alpha = 0$.

We now add a small ac signal $j_1(t)$ with frequency $\omega$ and consider how a small ac force $F_1(t)$ affects the vortex dynamics in the subcritical dc current regime, i.e., when $\tilde{j}_{0y} < j_c$. It follows from Eq. (20) that, when $j_1 = 0$, the value of $E_0$ can be obtained by averaging $\mathbf{E}_1(t)$ over time, taking into account the periodicity of $\mathbf{F}_1(t)$. Then $\mathbf{E} = \langle \mathbf{E}(t) \rangle$, where $\langle \ldots \rangle = 1/T \int_{t_0}^{t_0+T} \ldots dt$, and $T = 2\pi/\omega$. We note that $v_{0x} = 0$ when $j_{0y} < j_c$. As a result, one gets

$$\mathbf{E}_0 = \frac{nB}{c} v_{0y}\mathbf{x} = \frac{nB}{c}\frac{\gamma F_{0y}}{\eta_0}\mathbf{x}. \tag{31}$$

Here $F_{0y} = -n(\Phi_0/c)j_{0x}$, and therefore $\mathbf{E}_0 = -\gamma\rho_f j_{0x}\mathbf{x}$ and $E_{0x} = -\gamma\rho_f j_{0x}$.

It follows from Eq. (20) that

$$\begin{cases} E_{0\parallel} = E_{0x}\sin\alpha = -\gamma\rho_f j_0 \sin^2\alpha \equiv j_0\rho_{0\parallel}, \\ E_{0\perp} = -E_{0x}\cos\alpha = \gamma\rho_f j_0 \sin\alpha\cos\alpha \equiv j_0\rho_{0\perp}. \end{cases} \tag{32}$$

Finally,

$$\rho_{0\parallel} = -\gamma\rho_f \sin^2\alpha, \qquad \rho_{0\perp} = \gamma\rho_f \sin\alpha\cos\alpha, \tag{33}$$

from which it immediately follows that these responses are independent of the **B**-reversal. The only information which can be extracted from Eq. (33) is concerning the angle $\alpha$ for the given sample, from the relation $\tan\alpha = -\rho_{0\parallel}/\rho_{0\perp}$ and the value of the product $\gamma\rho_f$. From Eq. (33) it also follows that the longitudinal and transverse responses are nondissipative only when $\alpha = 0$; this is caused by the subcritical nature of the transport current. A dissipation arises when $\alpha \neq 0$ due to the appearance of a component of the driving force $F_{0y}$ that does not contain the Hall constant [see Eq. (29) for $V_{0y}$, taking into account that $V_{0x} = 0$] and is directed along the WPP channels. Thus, when $\tilde{F}_{0x} < F_c$, the vortex motion and the resistive response of the sample are independent of $\epsilon$, i.e., *the Hall parameter can not be determined from experiment at a constant subcritical current*, unlike the case already described in Sec. 4.2.1.

*4.3.2. Computing the ac impedance tensor*

Let us now proceed to an analysis of the responses to an ac current, using the relationship $\mathbf{E}_1(t) = \mathbf{E}(t) - \mathbf{E}_0 = \mathbf{E}(t) - \langle\mathbf{E}(t)\rangle$. From this and from Eq. (4) one has that

$$\begin{cases} \gamma v_{1x}(t) + \delta v_{1y}(t) = [\tilde{F}_{0x} + F_{1x}(t) + F_{px}]/\eta_0, \\ v_{1y}(t)/\gamma - \delta v_{1x}(t) = F_{1y}(t)/\eta_0, \end{cases} \tag{34}$$

where $F_{1x}(t) \equiv (n\Phi_0/c)j_{1y}(t)$ and $F_{1y}(t) \equiv -(n\Phi_0/c)j_{1x}(t)$, where $j_{1x}(t) = j_1(t)\sin\alpha$, $j_{1y}(t) = j_1(t)\cos\alpha$, and $j_1(t) = j_1 \exp i\omega t$. We use the fact that $\tilde{F}_{0x} + F_{px} \equiv \tilde{F}_{px} = -d\tilde{U}_p(x)/dx$, where $\tilde{U}_p(x) \equiv U_p(x) - x\tilde{F}_{0x}$ is the effective PP, taking into account the driving force component along the $x$ axis (see Fig. 4). In this case, the rest coordinate for a vortex is given by Eq. (30). The effective PP $\tilde{U}_p(x)$ can be expanded in series in the small difference $(x - x_0)$ like it was done in Sec. 3.2, and using Eq. (30) one gets

$$\tilde{F}_{px}/\eta_0 = -\tilde{\omega}_p(x - x_0), \quad \text{where} \quad \tilde{\omega}_p = \omega_p\sqrt{1 - (\tilde{j}_{0y}/j_c)^2}, \quad \text{and} \quad \omega_p \equiv k_p/\eta_0. \tag{35}$$

Now it is possible to rewrite Eq. (34) as

$$\begin{cases} (\gamma + \tilde{\omega}_p/i\omega)v_{1x}(t) + \delta v_{1y}(t) = F_{1x}(t)/\eta_0, \\ -\delta v_{1x}(t) + (1/\gamma)v_{1y}(t) - \delta v_{1x}(t) = F_{1y}(t)/\eta_0. \end{cases} \tag{36}$$

The solution of this system of equation is

$$v_{1x}(t) = (F_{1x}/\gamma - \delta F_{1y})/(\eta_0\Delta_\gamma), \qquad v_{1y}(t) = [\gamma F_{1y}(1 + \tilde{\omega}_{p\gamma}/i\omega) + \delta F_{1x}]/(\eta_0\Delta_\gamma), \tag{37}$$

where $\tilde{\omega}_{p\gamma} \equiv \tilde{\omega}_p/\gamma$ and $\Delta_\gamma \equiv \Delta + \tilde{\omega}_{p\gamma}/i\omega$. From the relation $\mathbf{E}_1(t) = \hat{Z}\mathbf{j}_1(t)$, where the components of the ac impedance tensor $\hat{Z}$ are measured in the $xy$ coordinate system (see Fig. 2), Eqs. (4), and (37), the longitudinal and transverse (with respect to the direction of $\mathbf{j}_1$) impedances $Z_\parallel$ and $Z_\perp$ are determined as

$$\begin{cases} Z_\parallel = (\rho_f/\gamma\Delta)[\gamma^2(\Delta - \delta^2 Z_1)\sin^2\alpha + Z_1\cos^2\alpha], \\ Z_\perp = (\rho_f/\gamma\Delta)\{\delta\gamma Z_1 + [Z_1 - \gamma^2(\Delta - \delta^2 Z_1)\sin\alpha\cos\alpha]\}, \end{cases} \tag{38}$$

where $Z_1 \equiv \Delta/\Delta_\gamma = 1/(1 - i\omega_q/\omega)$, and

$$\omega_q = \tilde{\omega}_{p\gamma}/\Delta = [\omega_p/\gamma\Delta]\sqrt{1-(\tilde{j}_{0y}/j_c)^2} = [\omega_p/\gamma\Delta]\sqrt{1-(j_{0y}/j_c)^2(\cos\alpha + \delta\gamma\sin\alpha)^2} \quad (39)$$

The quantity $\omega_q$ in Eq. (39) a generalization to the case $\gamma \neq 1$ and $\epsilon \neq 0$, and is physically analogous to the depinning frequency $\omega_p$ introduced in Seq. 3.1 and dependent on the subcritical transport current. However, it should be emphasized that, unlike the depinning frequency $\omega_p$ which is independent on the **B**-inversion, the value of the $\omega_q$ changes with the replacement $n \to -n$, i.e., $\delta \to -\delta$ because the Hall effect is present.

Having separated even and odd parts in the impedance components, finally the experimentally deducible, field orientation-independent quantities are

$$\begin{cases} Z_\parallel^+ = (\rho_f/\gamma\Delta)[\gamma^2(\Delta - \delta^2 Z_1^+)\sin^2\alpha + Z_1^+\cos^2\alpha], \\ Z_\parallel^- = (\rho_f/\gamma\Delta)Z_1^-(\cos^2\alpha - \delta^2\gamma^2\sin^2\alpha), \\ Z_\perp^+ = (\rho_f/\gamma\Delta)\{Z_1^+ - \gamma^2(\Delta - \delta^2 Z_1^+)]\sin\alpha\cos\alpha\}, \\ Z_\perp^- = (\rho_f/\gamma\Delta)\{\delta\gamma Z_1^+ + Z_1^-(1+\delta^2\gamma)\sin\alpha\cos\alpha\}, \end{cases} \quad (40)$$

*4.3.3. Determination of the Hall constant from microwave measurements*

Let us assume that $\gamma = 1$ and the Hall constant is arbitrary but satisfies the condition $\tilde{F}_{0x} < F_c$. Then $\bar{Z}_1 \equiv Z_1(\gamma = 1) = 1/(1 - i\bar{\omega}_q/\omega)$, where $\bar{\omega}_q \equiv (\omega_p/\Delta)\sqrt{1-(j_0/j_c)^2(\cos\alpha + \delta\sin\alpha)^2}$. In this case, the expressions for the real part of the longitudinal and transverse impedances $\mathrm{Re}\bar{Z}_{\parallel,\perp}$ are determined by

$$\begin{cases} \mathrm{Re}\bar{Z}_\parallel = (\rho_f/\Delta)[\mathrm{Re}\bar{Z}_1 + \Delta(1 - \mathrm{Re}\bar{Z}_1)\sin^2\alpha], \\ \mathrm{Re}\bar{Z}_\perp = (\rho_f/\Delta)[\delta\mathrm{Re}\bar{Z}_1 - \Delta(1 - \mathrm{Re}\bar{Z}_1)\sin\alpha\cos\alpha], \end{cases} \quad (41)$$

where $\mathrm{Re}\bar{Z}_1 = 1/[1 + (\bar{\omega}_q/\omega)^2]$.

The culmination of this subsection is an analysis of the dependence $\mathrm{Re}\bar{Z}_{\parallel,\perp}^{\pm}$ as a function of $\omega$ at large or small frequencies. If $\omega \to \infty$, one has $(\bar{\omega}_q/\omega) \to 0$, i.e., $\mathrm{Re}\bar{Z}_1 = 1$. Then in the main approximation with respect to $1/\omega$ one has $\mathrm{Re}\bar{Z}_\parallel = \rho_f/\Delta$, (i.e., $\mathrm{Re}\bar{Z}_\parallel^+ = \mathrm{Re}\bar{Z}_\parallel$ and $\mathrm{Re}\bar{Z}_\parallel^- = 0$), and $\mathrm{Re}\bar{Z}_\perp = \rho_f\delta/\Delta$, i.e., $\mathrm{Re}\bar{Z}_\perp^+ = 0$ and $\mathrm{Re}\bar{Z}_\perp^- = \mathrm{Re}\bar{Z}_\perp$. Thus, as the Hall constant $\epsilon$ increases (i.e., $\delta$ increases), the absorbed power $P$ decreases as $\omega \to \infty$ ($P = P_0/\Delta$). Moreover, as $\omega \to \infty$, for any $\alpha$, there is a relationship of the form $\delta = \mathrm{Re}\bar{Z}_\perp^-/\mathrm{Re}\bar{Z}_\parallel^-$. Now let $\omega \to 0$ (i.e., $\mathrm{Re}\bar{Z}_1 = 1$). Then, in the main approximation with respect to $\omega$, the Hall effect is unmeasurable, since $\mathrm{Re}\bar{Z}_\parallel = \rho_f\sin^2\alpha$ and $P = P_0\sin^2\alpha$, while $\mathrm{Re}\bar{Z}_\perp = -\rho_f\sin\alpha\cos\alpha$; i.e., $\delta$ has been canceled out of the results. It follows from this that $\rho_f = \mathrm{Re}\bar{Z}_\parallel/\sin^2\alpha$; i.e., $\eta_0 = B\Phi_0\sin^2\alpha/\mathrm{Re}\bar{Z}_\parallel c^2$.

Thus, the high-frequency limit $\omega \gg \bar{\omega}_q$ ($\omega \to \infty$) is needed to determine $\epsilon = \alpha_H/\eta_0$, whereas the low-frequency limit $\omega \ll \bar{\omega}_q$ ($\omega \to 0$) is sufficient to determine $\eta_0$. Because of the dependence $\bar{\omega}_q(j)$, appropriate measurements can be performed *even at one fixed frequency* $\omega \lesssim \omega_p$. Thus, for any $\epsilon$ and $\alpha = \pi/2$, the Hall constant in a periodic PP from microwave absorption by vortices is determined by

$$\alpha_H = (B\Phi_0/\bar{\rho}(0)c^2\sqrt{\bar{\rho}(0)/\bar{\rho}(\infty) - 1}, \tag{42}$$

where $\bar{\rho}(0) = \rho_f \sin^2\alpha$ for $\omega \to 0$ and $\bar{\rho}(\infty) = \rho_f/\Delta$ for $\omega \to \infty$.

*4.3.4. Microwave absorption by vortices in a washboard pinning potential*

By analogy with Sec. 4.2.4, the absorbed power is $P = (j_1^2/2)\mathrm{Re}Z_{\parallel} \equiv (j_1^2/2)\bar{\rho}$, where now

$$\bar{\rho} = (\rho_f/\gamma\Delta)\{\Delta\gamma^2 \sin^2\alpha + [1 - (1 + \delta^2\gamma^2)\sin^2\alpha]\mathrm{Re}Z_1\} \tag{43}$$

If $\delta = 0$ and $\gamma = 1$, Eq. (43) reduces to $\bar{\rho} = \rho_f(\sin^2\alpha + \mathrm{Re}Z_1 \cos^2\alpha)$ which has been dealt with previously [50]. Let $Z_1 \equiv 1 - iG_1$, where $G_1 = -(\omega_q/\omega)/(1 - i\omega_q/\omega)$, and consequently $\mathrm{Re}Z_1 = 1 - \mathrm{Re}(iG_1) = 1 + \mathrm{Im}G_1$. Then from Eq. (43) one has that

$$\bar{\rho} = (\rho_f/\gamma\Delta)\{\gamma^2 \sin^2\alpha + \cos^2\alpha + [1 - (1 + \delta^2\gamma^2)\sin^2\alpha]\mathrm{Im}G_1\} \tag{44}$$

where $\mathrm{Im}G_1 = -1/[1 + (\omega/\omega_q)^2]$. When $\gamma = 1$, Eq. (44) reduces to Eq. (85) in our previous work [25]. Finally,

$$P = P_0\{1 + (\gamma^2 - 1)\sin\alpha + [1 - (1 + \delta^2\gamma^2)\sin^2\alpha]\mathrm{Im}G_1\}/\gamma\Delta, \tag{45}$$

where $P_0 = \rho_f(j_1^2/2)/$ Unlike the case in which is no pinning (Sec. 4.2.4), the absorbed power $P$ in this case not only depends on angle $\alpha$, anisotropy parameter $\gamma$, and Hall constant $\epsilon$, but also depends on frequency $\omega$ and current density $j_0$.

It is essential to point out, that in that case under consideration, the absorbed power contains both even and odd parts with regards to the change $\mathbf{B} \to -\mathbf{B}$; this is because of the dependence of $\mathrm{Im}G_1$ through $\omega_q$ on $n$ [see Eq. (39)]. Thus, the experimentally observed $P(B)$ changes under the reversal of the direction of $\mathbf{B}$. Therefore, it is convenient to represent the absorbed power as $P(B) = P^+(B) + P^-(B)$, where $P^{\pm}(B) \equiv [P(B) \pm P(-B)]/2$ are moduli that do not change their quantities under inversion of $\mathbf{B}$.

## 5. Conclusion

### 5.1. Summary

The microwave absorbtion by vortices in a superconductor with a periodic (washboard-type) pinning potential in the presence of the Hall effect and viscosity anisotropy has been studied theoretically. Two groups of results have been discussed. First, it has been shown how the Gittleman-Rosenblum model can be generalized for the case when a subcritical dc current is superimposed on a weak ac current. It has been elucidated how the coordinate dependence

of a pinning potential can be reconstructed from the microwave absorption data measured at a set of subcritical dc currents. Second, the dependences of the longitudinal and transverse dc resistivity and ac impedance tensors, as well as of the absorbed power on the subcritical constant current density $j_0$, the ac frequency $\omega$, the dimensionless Hall parameter $\delta$, the anisotropy coefficient $\gamma$, and the angle $\alpha$ between the direction of the collinear currents $j_0$ and $j_1(t)$ with respect to the channels of the WPP have been derived for the general case. The physics of the vortex motion in a pinning potential subjected to superimposed dc an ac drives has been elucidated. In particular, it has been shown that the results are most substantially affected not by the value of $\gamma$ but by the value of the Hall parameter $\epsilon$. At a constant subcritical current $j_0 < j_c$, it turns out that $\epsilon$ does not appear in the resistive responses, whereas, at a small ac current, two new effects result from the presence of $\epsilon$, namely (i) a falloff of the absorbtion as $\epsilon$ increases at any subcritical current $j_0 < j_c$, and (ii) the appearance of an odd-in-field component $P^-(\omega)$ when $\alpha \neq 0; 90$, and this increases with increasing $\epsilon$.

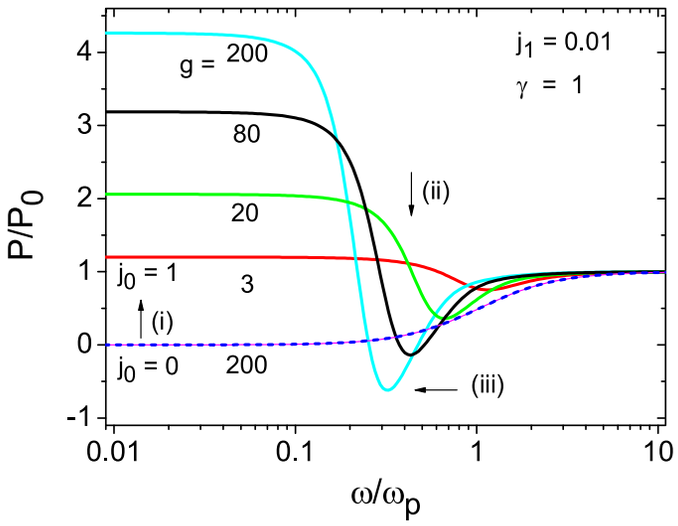


**Figure 8.** Dependence of the absorbed power $P/P_0$ on the dimensionless frequency $\omega/\omega_p$ calculated on the basis of a stochastic model [25]. In the presence of a dc current $j_0 = 1$ and a series of dimensionless inverse temperatures $g = U_p/2T$, as indicated, $P(\omega)$ demonstrates (i) an enhanced power absorption by vortices at low frequencies, (ii) a pronounced temperature-dependent minimum at intermediate frequencies and (iii) a sign change at certain conditions [27]. Experimentally, $U_0 \simeq 1000 \div 5000$ K typically [10], and $\omega_p$ usually ensues in the microwave range [16, 30, 42]. In the limit of zero dc current $j_0 = 0$, the curves coincide with the well-known results of Coffey and Clem (dashed line) [49].

Our discussion has been limited by the consideration of $j_0 < j_c$ and $j_1 \to 0$ mainly for two reasons. First, at a steady-state dc current $j_0 > j_c$ the dissipated power $P_0 \sim \rho_f j_0^2$ may be significant and because of this the *overheating* of the sample is unavoidable and as a result the heat release in the film should be properly analyzed. We note, however, this difficulty can be overcome provided high-speed current sweeps [59] or short-pulse measurements [60] are employed. The second reason is that at $j_0 > j_c$ a *running* mode in the vortex dynamics appears [25], when the vortex moves in a tilted WPP with instantaneous velocity oscillating with frequency $\omega_i$. Due to the presence of the two frequencies, i.e., *intrinsic* $\omega_i$ and *external* $\omega$, the problem of their synchronization arises. Though an analytical treatment of this issue could be presented, to work out a clear physical picture for this problem would be more complicate.

### 5.2. Extension of the theory for non-zero temperature

Finally, let us compare the results presented in the chapter with the analogous but more general results obtained by the authors [25] on the basis of a stochastic model for arbitrary temperature $T$ and densities $j_0$ and $j_1$. In that work, the Langevin equation (1), supplemented with a thermofluctuation term, has been *exactly* solved for $\gamma = 1$ in terms of a matrix continued fraction [52] and, depending on the WPP's tilt caused by the dc current, two substantially different modes in the vortex motion have been predicted. In more detail, at low temperatures and relatively high frequencies in a *nontilted* pinning potential each pinned vortex is *confined* to its pinning potential well during the *ac* period. In the case of superimposed strong ac and dc driving currents a *running* state of the vortex may appear when it can visit several (or many) potential wells during the ac period. As a result, two branches of new findings have been elucidated [25, 27]. First, the influence of an ac current on the usual $E_0(j_0)$ and ratchet $E_0(j_1)$ CVCs has been analyzed. Second, the influence of a dc current on the ac nonlinear impedance response and nonlinear power absorption has been investigated. In particular, the appearance of Shapiro-like steps in the usual CVC and the appearance of phase-locking regions in the ratchet CVC has been predicted. At the same time, it has been shown that an anomalous power absorption in the ac response is expected at close-to critical currents $j_0 \simeq j_c$ and relatively low frequencies $\omega \lesssim \omega_p$. Figure 8 shows the main predictions of these works. Namely, predicted are (i) an enhanced power absorption at low frequencies, (ii) a temperature- and current-dependent minimum at intermediate frequencies. (iii) At substantially low temperatures, the absorption can acquire negative values which physically corresponds to the generation by vortices. However, a more general and formally precise solution of the problem in terms of a matrix-continued fraction does not allow the main physical results of the problem to be investigated in the form of explicit analytical functions of the main physical quantities ($j_0$, $j_1$, $\omega$, $\alpha$, $T$, $\epsilon$, and $\gamma$) which, we believe, has helped us greatly to elucidate the physics in the problem under consideration.

## Acknowledgements

The authors are very grateful to Michael Huth for useful comments and critical reading. O.V.D. gratefully acknowledges financial support by the Deutsche Forschungsgemeinschaft (DFG) through Grant No. DO 1511/2-1.

## Author details

Valerij A. Shklovskij
*Institute of Theoretical Physics, NSC-KIPT, 61108 Kharkiv*
*Physical Department, Kharkiv National University, 61077 Kharkiv, Ukraine*

Oleksandr V. Dobrovolskiy
*Physikalisches Institut, Goethe-University, 60438 Frankfurt am Main, Germany*

## 6. References

[1] L. V. Shubnikov, V. I. Khotkevich, Yu. D. Shepelev, and Yu. N. Ryabinin. Magnetic properties of superconductors and alloys. *Zh. Eksper. Teor. Fiz.*, 7:221–237, 1937.

[2] L. V. Shubnikov, V. I. Khotkevich, Yu. D. Shepelev, and Yu. N. Ryabinin. Magnetic properties of superconductors and alloys. *Ukr. J. Phys.*, 53:42–52, 2008.
[3] A. A. Abrikosov. On the magnetic properties of second kind superconductors. *Sov. Phys. JETP.*, 5:1174–1182, 1957.
[4] Ernst Helmut Brandt. The flux-line lattice in superconductors. *Rep. Progr. Phys.*, 58:1465–1594, 1995.
[5] A. V. Silhanek, J. Van de Vondel, and V. V. Moshchalkov. *Guided Vortex Motion and Vortex Ratchets in Nanostructured Superconductors*, chapter 1, pages 1–24. Springer-Verlag, Berlin Heidelberg, 2010.
[6] G. Blatter, M. V. Feigel'man, V. B. Geshkenbein, A. I. Larkin, and V. M. Vinokur. Vortices in high-temperature superconductors. *Rev. Mod. Phys.*, 66:1125–1388, Oct 1994.
[7] P. W. Anderson. Theory of flux creep in hard superconductors. *Phys. Rev. Lett.*, 9:309–311, Oct 1962.
[8] Ivar Giaever. Magnetic coupling between two adjacent type-ii superconductors. *Phys. Rev. Lett.*, 15:825–827, Nov 1965.
[9] A.T. Fiory, A. F. Hebard, and S. Somekh. Critical currents associated with the interaction of commensurate fluxline sublattices in a perforated al film. *Appl. Phys. Lett.*, 32:73–75, Jan 1978.
[10] Oleksiy K. Soroka, Valerij A. Shklovskij, and Michael Huth. Guiding of vortices under competing isotropic and anisotropic pinning conditions: Theory and experiment. *Phys. Rev. B*, 76:014504, Jul 2007.
[11] O. V. Dobrovolskiy, M. Huth, and V. A. Shklovskij. Anisotropic magnetoresistive response in thin nb films decorated by an array of co stripes. *Supercond. Sci. Technol.*, 23(12):125014, 2010.
[12] Valerij A. Shklovskij and Oleksandr V. Dobrovolskiy. Influence of pointlike disorder on the guiding of vortices and the hall effect in a washboard planar pinning potential. *Phys. Rev. B*, 74:104511, Sep 2006.
[13] O. K. Soroka. *Vortex dynamics in superconductors in the presence of anisotropic pinning*. PhD thesis, Johannes Gutenberg University, 2005.
[14] A. K. Niessen and C. H. Weijsenfeld. Anisotropic pinning and guided motion of vortices in type-ii superconductors. *J. Appl. Phys.*, 40:384–394, 1969.
[15] R Wördenweber, J. S. K. Sankarraj, P. Dymashevski, and E. Holmann. Anomalous hall effect studied via guided vortex motion. *Physica C*, 434:1010–104, 2006.
[16] E. Silva, N. Pompeo, S. Sarti, and C. Amabile. *Vortex State Microwave Response in Superconducting Cuprates*, chapter 1, pages 201–243. Nova Science, Hauppauge, NY, 2006.
[17] C. S. Lee, B. Janko, I. Derenyi, and A. L. Barabasi. Reducing vortex density in superconductors using the 'ratchet effect'. *Nature*, 400:337–340, May 1999.
[18] B. L. T. Plourde. Nanostructured superconductors with asymmetric pinning potentials: Vortex ratchets. *IEEE Trans. Appl. Supercond.*, 19:3698 – 3714, Oct 2009.
[19] Peter Hänggi and Fabio Marchesoni. Artificial brownian motors: Controlling transport on the nanoscale. *Rev. Mod. Phys.*, 81:387–442, Mar 2009.
[20] R. Wördenweber, P. Dymashevski, and V. R. Misko. Guidance of vortices and the vortex ratchet effect in high-$T_c$ superconducting thin films obtained by arrangement of antidots. *Phys. Rev. B*, 69:184504, May 2004.

[21] A. Crisan, A. Pross, D. Cole, S. J. Bending, R. Wördenweber, P. Lahl, and E. H. Brandt. Anisotropic vortex channeling in YBaCuO thin films with ordered antidot arrays. *Phys. Rev. B*, 71:144504, Apr 2005.

[22] J. E. Villegas, K. D. Smith, Lei Huang, Yimei Zhu, R. Morales, and Ivan K. Schuller. Switchable collective pinning of flux quanta using magnetic vortex arrays: Experiments on square arrays of co dots on thin superconducting films. *Phys. Rev. B*, 77:134510, Apr 2008.

[23] J. I. Martin, Y. Jaccard, A. Hoffmann, J. Nogues, J. M. George, J. L. Vicent, and I. K. Schuller. Fabrication of submicrometric magnetic structures by electron-beam lithography. *J. Appl. Phys.*, 434:411–416, 1998.

[24] V. A. Shklovskij, A. K. Soroka, and A. A. Soroka. Nonlinear dynamics of vortices pinned to unidirectional twins. *J. Exp. Theor. Phys.*, 89:1138–1153, 1999.

[25] Valerij A. Shklovskij and Oleksandr V. Dobrovolskiy. ac-driven vortices and the hall effect in a superconductor with a tilted washboard pinning potential. *Phys. Rev. B*, 78:104526, Sep 2008.

[26] Valerij A. Shklovskij and Vladimir V. Sosedkin. Guiding of vortices and ratchet effect in superconducting films with asymmetric pinning potential. *Phys. Rev. B*, 80:214526, Dec 2009.

[27] Valerij A. Shklovskij and Oleksandr V. Dobrovolskiy. Frequency-dependent ratchet effect in superconducting films with a tilted washboard pinning potential. *Phys. Rev. B*, 84:054515, Aug 2011.

[28] Valerij A. Shklovskij. Guiding of vortices and the hall conductivity scaling in a bianisotropic planar pinning potential. *Phys. Rev. B*, 65:092508, Feb 2002.

[29] M. Huth, K.A. Ritley, J. Oster, H. Dosch, and H. Adrian. Highly ordered Fe and Nb stripe arrays on facetted $\alpha - al_2o_3$ $(10\bar{1}0)$. *Adv. Func. Mat.*, 12(5):333–338, 2002.

[30] Jonathan I. Gittleman and Bruce Rosenblum. Radio-frequency resistance in the mixed state for subcritical currents. *Phys. Rev. Lett.*, 16:734–736, Apr 1966.

[31] D. D. Morrison and R. M. Rose. Controlled pinning in superconducting foils by surface microgrooves. *Phys. Rev. Lett.*, 25:356–359, Aug 1970.

[32] D. Jaque, E. M. Gonzalez, J. I. Martin, J. V. Anguita, and J. L. Vicent. Anisotropic pinning enhancement in Nb films with arrays of submicrometric Ni lines. *Appl. Phys. Lett.*, 81:2851 – 2854, Oct 2002.

[33] Y Yuzhelevski and G. Jung. Artificial reversible and programmable magnetic pinning for high-$T_c$ superconducting thin films. *Physica C: Superconductivity*, 314(314):163 – 171, 1999.

[34] O. V. Dobrovolskiy, E. Begun, M. Huth, and V. A. Shklovskij. private communication. 2012.

[35] T. A. Friedmann, M. W. Rabin, J. Giapintzakis, J. P. Rice, and D. M. Ginsberg. Direct measurement of the anisotropy of the resistivity in the ab plane of twin-free, single-crystal, superconducting $YBa_2Cu_3O_{7-\delta}$. *Phys. Rev. B*, 42:6217–6221, Oct 1990.

[36] Y. Matsuda, N. P. Ong, Y. F. Yan, J. M. Harris, and J. B. Peterson. Vortex viscosity in $YBa_2Cu_3O_{7-\delta}$ at low temperatures. *Phys. Rev. B*, 49:4380–4383, Feb 1994.

[37] P. Berghuis, E. Di Bartolomeo, G. A. Wagner, and J. E. Evetts. Intrinsic channeling of vortices along the *ab* plane in vicinal $YBa_2Cu_3O_{7-\delta}$ films. *Phys. Rev. Lett.*, 79:2332–2335, Sep 1997.

[38] H. Pastoriza, S. Candia, and G. Nieva. Role of twin boundaries on the vortex dynamics in $YBa_2Cu_3O_{7-\delta}$. *Phys. Rev. Lett.*, 83:1026–1029, Aug 1999.

[39] G. D'Anna, V. Berseth, L. Forró, A. Erb, and E. Walker. Scaling of the hall resistivity in the solid and liquid vortex phases in twinned single-crystal $YBa_2Cu_3O_{7-\delta}$. *Phys. Rev. B*, 61:4215–4221, Feb 2000.

[40] V. A. Shklovskij. Hot electrons in metals at low temperatures. *Journal of Low Temperature Physics*, 41:375–396, 1980. 10.1007/BF00117947.

[41] A. I. Bezuglyj and V. A. Shklovskij. Effect of self-heating on flux flow instability in a superconductor near $T_c$. *Physica C: Superconductivity*, 202:234 – 242, 1992.

[42] B. B. Jin, B. Y. Zhu, R. Wördenweber, C. C. de Souza Silva, P. H. Wu, and V. V. Moshchalkov. High-frequency vortex ratchet effect in a superconducting film with a nanoengineered array of asymmetric pinning sites. *Phys. Rev. B*, 81:174505, May 2010.

[43] C. Song, M. P. DeFeo, and B. L. T. Yu, K. Plourde. Reducing microwave loss in superconducting resonators due to trapped vortices. *Appl. Phys. Lett.*, 95:232501, 2009.

[44] N. S. Lin, T. W. Heitmann, K. Yu, B. L. T. Plourde, and V. R. Misko. Rectification of vortex motion in a circular ratchet channel. *Phys. Rev. B*, 84:144511, Oct 2011.

[45] N. Pompeo, E. Silva, S. Sarti, C. Attanasio, and C. Cirillo. New aspects of microwave properties of nb in the mixed state. *Physica C: Superconductivity*, 470(19):901 – 903, 2010.

[46] D. Janjušević, M. S. Grbić, M. Požek, A. Dulčić, D. Paar, B. Nebendahl, and T. Wagner. Microwave response of thin niobium films under perpendicular static magnetic fields. *Phys. Rev. B*, 74:104501, Sep 2006.

[47] V. A. Shklovskij and O. V. Dobrovolskiy. private communication. 2012.

[48] Jonathan I. Gittleman and Bruce Rosenblum. The pinning potential and high-frequency studies of type-ii superconductors. *J. Appl. Phys.*, 39(6):2617–2621, 1968.

[49] Mark W. Coffey and John R. Clem. Unified theory of effects of vortex pinning and flux creep upon the rf surface impedance of type-ii superconductors. *Phys. Rev. Lett.*, 67:386–389, Jul 1991.

[50] V. A. Shklovskij and Dang Thi Bich Hop. Effect of the transport current on microwave absorption by vortices in type-ii superconductors. *Low Temp. Phys.*, 35(5):365 – 369, 2009.

[51] V. A. Shklovskij and Dang Thi Bich Hop. The hall effect and microwave absorption by vortices in an anisotropic superconductor with a periodic pinning potential. *Low Temp. Phys.*, 36(71):71 – 80, 2010.

[52] W. T. Coffey, J. L. Déjardin, and Yu. P. Kalmykov. Nonlinear impedance of a microwave-driven josephson junction with noise. *Phys. Rev. B*, 62:3480–3487, Aug 2000.

[53] Yasunori Mawatari. Dynamics of vortices in planar pinning centers and anisotropic conductivity in type-ii superconductors. *Phys. Rev. B*, 56:3433–3437, Aug 1997.

[54] Yasunori Mawatari. Anisotropic current-voltage characteristics in type-ii superconductors with planar pinning centers. *Phys. Rev. B*, 59:12033–12038, May 1999.

[55] G. Grüner. The dynamics of charge-density waves. *Rev. Mod. Phys.*, 60:1129–1181, Oct 1988.

[56] A. A. Golubov, M. Yu. Kupriyanov, and E. Il'ichev. The current-phase relation in josephson junctions. *Rev. Mod. Phys.*, 76:411–469, Apr 2004.

[57] A. M. Campbell and J. E. Evetts. Flux vortices and transport currents in type ii superconductors. *Adv. Phys.*, 21(90):199–428, 1972.

[58] J. M. Harris, Y. F. Yan, O. K. C. Tsui, Y. Matsuda, and N. P. Ong. Hall angle evidence for the superclean regime in 60 k $YBa_2Cu_3O_{6+y}$. *Phys. Rev. Lett.*, 73:1711–1714, Sep 1994.
[59] A. Leo, G. Grimaldi, R. Citro, A. Nigro, S. Pace, and R. P. Huebener. Quasiparticle scattering time in niobium superconducting films. *Phys. Rev. B*, 84:014536, Jul 2011.
[60] Manlai Liang and Milind N. Kunchur. Vortex instability in molybdenum-germanium superconducting films. *Phys. Rev. B*, 82:144517, Oct 2010.



IntechOpen